HiSST: 4th International Conference on High-Speed Vehicle Science Technology
22 -26 September 2025, Tours, France

Experiments on High-Speed Air-Breathing Propulsion with Different Fuels for Sustainable Supersonic Flight

Friedolin T. Strauss[1], Luca Bauer[2], Nico Fischer[3], Samuel Michelfelder[4], Christoph Kirchberger[5]

Abstract

This publication presents selected results of an investigation into combustion processes and environmental impacts of ramjets and scramjets at the German Aerospace Center (DLR) within the European MORE&LESS project. It compares typical chemical exhaust gas compositions for the liquid hydrocarbon-based fuels tested, including pure laboratory hydrocarbons and so-called bio fuel / sustainable aviation fuel at a similar mass flow rate. Additionally, the static wall temperature and static wall pressure distributions for two different positions at the cavity injector are analysed for hydrocarbon-based fuels and gaseous hydrogen for comparison. Each of the different fuels shows a unique behaviour in terms of flame / combustion zone position and effect on the wall pressure distribution. In general, the influence of the flame zone on the wall pressure decreases with increasing stagnation pressure of the test bench. In contrast the wall temperature increases with increasing stagnation pressure as more oxidiser from the hot gas main flow becomes available to the combustion process. The results correspond to the numerical simulations of project partners within More&Less in terms of flame position, but the findings need further detailed analysis.

Keywords: *Ramjet, Ground Testing, More&Less, Thermodynamics, Gasdynamics*

1. Introduction

Internationally, research on sustainable and efficient alternatives to current aerospace propulsion systems has increased demand for replacement of toxic propellants and for the modernization of existing systems through greater efficiency. These drivers along with national security challenges have brought ramjets with supersonic combustion (scramjets) and other systems back into focus (see e.g. [1]-[3]). The main challenges of high-speed air-breathing propulsion systems like ramjets and scramjets are short fuel residence times, controlled mixing and combustion, and efficient /sufficient cooling of the engine's components exposed to very high heat loads. However, in their practical application especially for future sustainable supersonic flight, the focus is also on the emissions generated by the propulsion system. This is a so far mostly neglected aspect of HSABP research and needs increasing attention. Thus, the project *MDO and REgulations for Low boom and Environmentally Sustainable Supersonic aviation (More&Less)* features a combination of high-fidelity simulation / modelling activities and test campaigns that merge into the multi-disciplinary optimization framework to assess the holistic impact of supersonic aviation onto environment. This ultimately leads to recommendations to shape European and global regulations for sustainable supersonic aviation. DLR Lampoldshausen is included in the project with its unique high-speed air-breathing propulsion testing capabilities to provide the necessary experimental testing data on ramjet propulsion. In summary more than 400 hot runs have been performed within this project using three different fuels, two hydrocarbons and gaseous hydrogen.

[1] *German Aerospace Center (DLR), D-74239 Hardthausen, Germany, Friedolin.Strauss@dlr.de*
[2] *German Aerospace Center (DLR), D-74239 Hardthausen, Germany, Luca.Bauer@dlr.de*
[3] *German Aerospace Center (DLR), D-74239 Hardthausen, Germany, Nico.Fischer@dlr.de*
[4] *German Aerospace Center (DLR), D-74239 Hardthausen, Germany, Samuel.Michelfelder@dlr.de*
[5] *German Aerospace Center (DLR), D-74239 Hardthausen, Germany, Christoph.Kirchberger@dlr.de*

2. Experimental Setup

The Institute of Space Propulsion of the German Aerospace Center (DLR) Lampoldshausen has established a research test bench (M11.1) to investigate high speed air-breathing propulsion (HSABP) and modified it for this project to collect data on its application in sustainable supersonic flight. The test bench (see [4], [5], [6] for details and performance) consists of a hydrogen / oxygen air vitiator (Fig. 1) with 11 hydrogen / oxygen burners that heat up the pressurized air fed through them. They can be interconnected in different burner patterns and equipped with different orifices to adjust the mass flow, pressure, and temperature of the vitiated air as required.

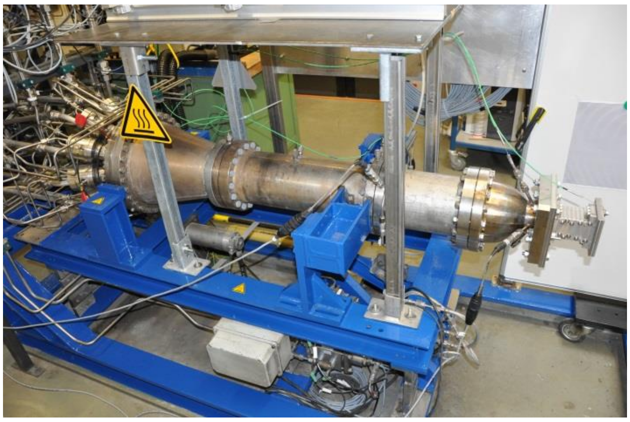

Fig 1. M11.1 Air Vitiator at DLR Lampoldshausen

It is possible to reach stagnation temperatures up to 1500 K, stagnation pressures of 25 to 30 bars and mass flows of 5,0 kg /s maximum with the air vitiator with testing time reaching from several seconds to several minutes. Connected to the air vitiator is a geometrical transition section that converts the round cross-section (diameter 135 mm) into a rectangular cross-section (45 by 45 mm) with minimal influence on the boundary layer

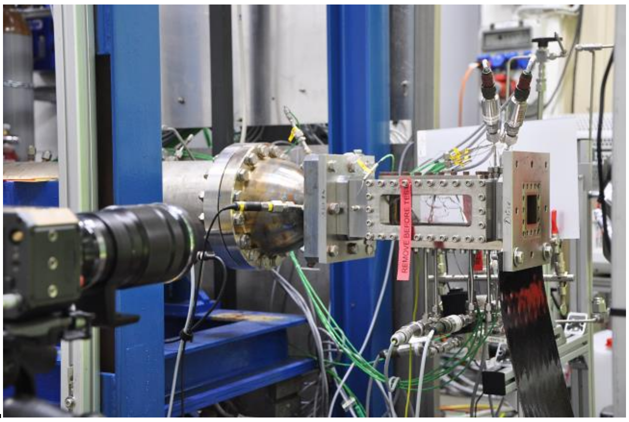

Fig 2. HSABP Model Combustion Chamber in Ramjet Configuration

For the More&Less project a model combustion chamber is connected to the previously mentioned transition section (Fig. 2). This versatile model combustion chamber (length 300 mm) can accommodate different injector configurations and various types of measurement equipment. It can be operated either as a Ramjet or as a Scramjet. Details on the standard intrusive and non-intrusive measurement equipment of the model combustion chamber can be found in [7]. The experiments for More&Less were mostly performed in the Ramjet configuration with some tests in Scramjet configuration for reference purposes. Two quartz glass windows provided optical access and allowed the use of a Background Oriented Schlieren (BOS) system [4], [8] where appropriate. This system features detailed Schlieren imagery and was shown in previous HSABP experiments to be less affected by changes in the refractive index of the quartz glass windows due to strong heating [4]. Two sophisticated gas sampling systems were installed to measure the chemical gas composition and the water vapor content of the gas. The first sampling position is located at the air vitiator in the settling section downstream of the burner cans. It provides data on the initial water vapor and NO_X content of the vitiated gas. This can be used in comparison to reference samples of the pressurized air supply to calculate the water vapor and NO_X generation by the vitiation process. The second sampling station is located downstream of the model combustion chamber in the exhaust plume (Fig. 3). It consists of a water-cooled sampling probe that can be moved in three directions within the exhaust gas stream via an automatic positioning system. Gas samples collected with the probe initially pass through a sampling chamber where NO_X measurements are performed in-line by an off-the-shelf sensor. This probe also features the option to perform solid mater measurements with a filter. After passing the NO_X measurement chamber the sample is collected in evacuated gas sample cylinders for further analysis at the physic-chemical lab of DLR Lampoldshausen. The system is automatically flushed with fresh sampling gas before a sample is routed to one of the sample cylinders and it can acquire multiple samples during a single air vitiator run. For reference this NO_X sensor was also installed upstream at the air vitiator's gas sampling port in order to measure the native NO_X concentration in the vitiated air directly downstream of the burners.

Fig 3. Exhaust Emission Gas Sampling Rig Installed at Test Bench M11.1

3. Experimental Methodology

In the Ramjet combustion experiments, a cavity style injector was used with a single injection element located parallel to the hot gas main flow and on the bottom wall (see Fig. 4). Experiments have been performed using gaseous hydrogen (see Fig. 5a) and [9]), n-heptane (see Fig. 5b) and DLR's SAF1 (see Fig. 5c) as fuels. DLR's SAF1 has been tested previously in different aircraft flight test campaigns (see [10]). Those fuels were injected at various fuel mass flow rates and at different air vitiator boundary conditions such as 900K and 1200 K stagnation temperature at different stagnation pressures (5, 7 and 9 bar respectively).

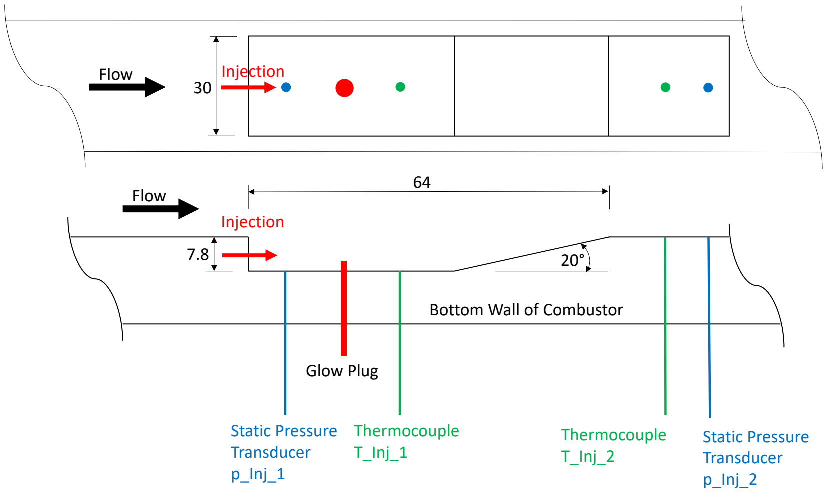

Fig 4. Scheme of DLR's cavity injector

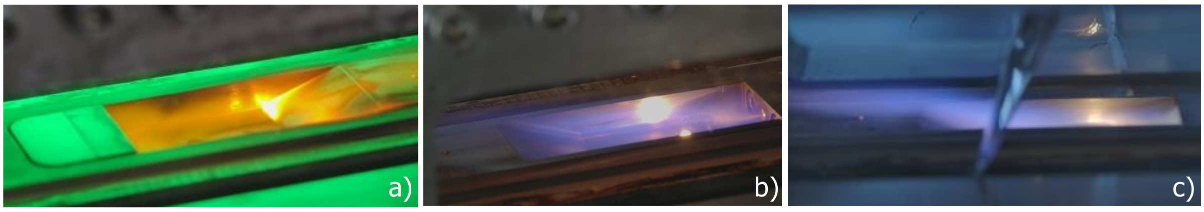

Fig 5. Combustion of different fuels in Ramjet configuration; a) Hydrogen, b) n-Heptane, c) SAF1

During the experiments a detailed understanding of the limits of air to fuel mixtures and limits of ignitability was obtained for all fuel types investigated. Some testing points showed self-sustaining combustion, others needed the constant help of a glowing plug as a heat source in order to push the limits of ignitability further (refer to [9] and [11]).

4. Results

In the Ramjet combustion experiments, a cavity style injector was used with a single injection element located parallel to the hot gas main flow and on the bottom

4.1. Exhaust Gas Composition

Tables 1 to 3 present the typical chemical composition of the exhaust gas as sampled with the downstream gas sampling setup described above. The tables compare the two liquid fuels n-Heptane and SAF for the same air vitiator boundary conditions and similar mass flow rates of 1.5 g/s and 1.6 g/s respectively for the centre position of the sampling probe (refer also to [11]). In Table 1 the exhaust composition of n-Heptane and SAF1 is compared with each other for the air vitiator boundary condition 5 bar / 1200 K. The adjusted amounts of the different species are very similar. However, for n-Heptane hydrogen could be detected in the exhaust gas, which was not the case for SAF. The amount of nitrogen is slightly lower for n-Heptane than for the SAF in the exhaust gas in contrast to the amount of CO_2, which is higher for n-Heptane. In reference measurements no unburned hydrogen could be found upstream at the air vitiator.

Table 1. Exhaust gas composition for 5 bar / 1200 K, fuel mass flow rate 1.5 g/s

	n-Heptane	**SAF**
Analysis Temperature [K]	294.00	294.20
Partial Pressure [mbar]	677.30	704.00
H_2 Adjusted Amount [mbar]	1.10	0.00
O_2 Adjusted Amount [mbar]	152.60	162.10
N_2 Adjusted Amount [mbar]	523.50	544.70
CO Adjusted Amount [mbar]	<0.10	0.00
CH_4 Adjusted Amount [mbar]	<0.10	0.00
Sum Adjusted Amount [mbar]	677.20	706.80
H_2 [Amount %]	0.16	0.00
O_2 [Amount %]	22.50	22.90
N_2 [Amount %]	77.30	77.10
CO [Amount %]	<0.10	0.00
CH_4 [Amount %]	<0.10	0.00
CO_2 [Amount %]	0.06	0.04
CO_2 [ppm]	611	373

Table 2. Exhaust gas composition for 7 bar / 1200 K, fuel mass flow rate 1,5 g/s

	n-Heptane	**SAF**
Analysis Temperature [K]	294.50	294.2
Partial Pressure [mbar]	780.00	723.00
H_2 Adjusted Amount [mbar]	1.10	0.00
O_2 Adjusted Amount [mbar]	173.90	164.40
N_2 Adjusted Amount [mbar]	607.00	558.4
CO Adjusted Amount [mbar]	<2.0	0.020
CH_4 Adjusted Amount [mbar]	<2.0	0.00
Sum Adjusted Amount [mbar]	782.00	722.80
H_2 [Amount %]	0.15	0.00
O_2 [Amount %]	22.20	22.70
N_2 [Amount %]	77.60	77.30
CO [Amount %]	0.00	0.00
CH_4 [Amount %]	0.00	0.00
CO_2 [Amount %]	0.06	0.05
CO_2 [ppm]	627	546

Table 2 shows the exhaust composition for the 1200 K / 7 bar boundary condition. As in the previous case for 1200 K and 5 bar, the n-Heptane samples contained hydrogen in contrast to the SAF gas samples. For this condition, the amount of produced CO2 is similar, whereas the nitrogen and oxygen amounts differ. Nitrogen content is lower for SAF whereas the oxygen amount is higher.

Table 3. Exhaust gas composition for 9 bar / 1200 K

	n-Heptane	**SAF**
Analysis Temperature [K]	293.90	294.20
Partial Pressure [mbar]	786.00	701.00
H_2 Adjusted Amount [mbar]	1.10	0.00
O_2 Adjusted Amount [mbar]	174.80	158.90
N_2 Adjusted Amount [mbar]	610.80	545.50
CO Adjusted Amount [mbar]	<2.0	0.01
CH_4 Adjusted Amount [mbar]	<2.0	0.00
Sum Adjusted Amount [mbar]	786.70	704.40
H_2 [Amount %]	0.14	0.00
O_2 [Amount %]	22.20	22.60
N_2 [Amount %]	77.60	77.40
CO [Amount %]	0.00	0.00
CH_4 [Amount %]	0.00	0.00
CO_2 [Amount %]	0.05	0.05
CO_2 [ppm]	493	485

If the stagnation temperature is further increased, the gas compositions changes only slightly (see Table 3). Also, in this case Hydrogen could be detected in the exhaust gas samples. The similar exhaust gas compositions at the centre line of the flow field show only a little effect of the intrusion depth of the hot gas into the cavity. The only major difference is the presence of hydrogen in the n-Heptane samples. Detailed NO_X measurements on the test runs of this publication can be found in [11].

4.2. Cavity Temperature and Pressure Distribution

Figure 6 shows the temperature distribution in the injection cavity (station "T_Inj_1" in Fig. 4) for the three different fuels and additionally the reference case without combustion. All three fuels were injected at similar fuel mass flow rates from 1.50 to 1.60 g/s and at the 5 bar / 1200 K air vitiator boundary condition for this comparison (see [11]). N-Heptane combustion causes the highest cavity temperature (1050 K). In case of SAF, the temperature reaches 780 K, whereas in contrast hydrogen reaches a temperature maximum of 675 K in the cavity. Without combustion the cavity temperature rises to 590 K instead.

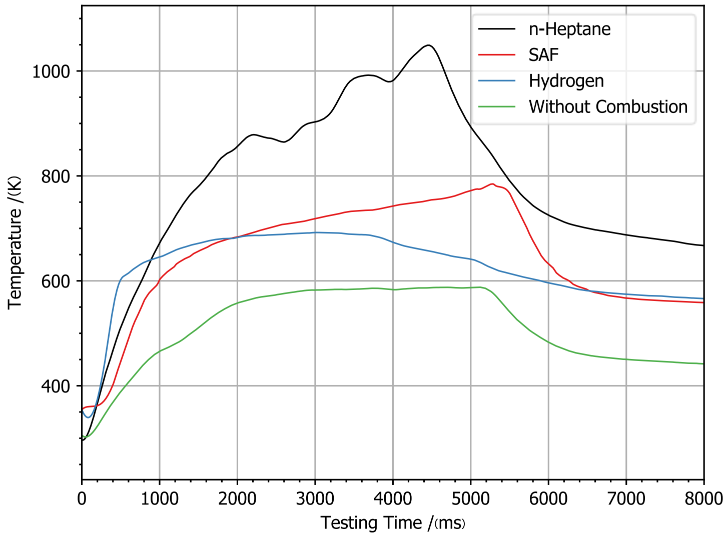

Fig 6. 5 bar / 1200 K, cavity temperature at station "T_Inj_1"

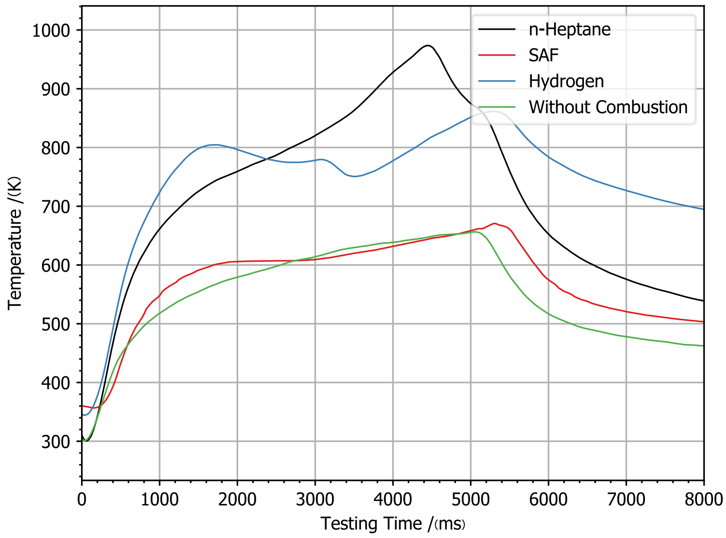

Fig 7. 5 bar / 1200 K, ramp temperature at station "T_Inj_2"

Figure 7 displays the temperatures for the three different fuels and the reference case without combustion at station "T_Inj_2" (see Fig. 4). This thermocouple station is located just downstream of the injector ramp. Without combustion the temperature is slightly higher than in the cavity (maximum around 650 K). That is caused by the location in proximity to the hot gas main flow with a similar static wall temperature. For SAF the maximum temperature is 680 K, close to the case without combustion. This indicates that the flame and combustion zone is located almost entirely in the cavity for this fuel. The temperature maximum for n-heptane reaches 980 K which is 70 K lower than in the cavity (refer to Fig. 6). Therefore, the flame position and the combustion zone are spread from the cavity to the ramp with a main zone slightly downstream. In contrast to Fig. 6 the graph shows less temperature fluctuations which supports the indication of the flame at a slightly downstream position. Hydrogen reaches a static temperature of about 900 K at the station "T_Inj_2" which is 250 K higher than in Fig. 5. Thus, the hydrogen combustion zone is located almost entirely at the ramp. At the end of the test run the temperature difference between the cavity and the ramp reaches its maximum with a cavity wall temperature almost at the level of the case without combustion and a temperature maximum at the ramp.

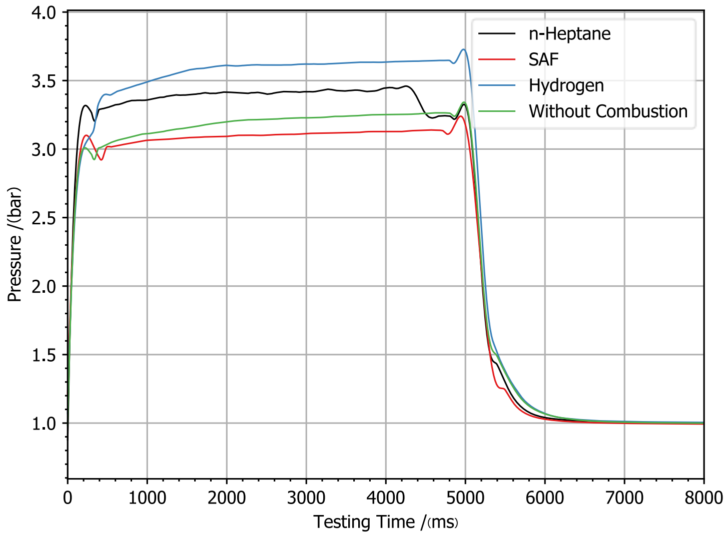

Fig 8. 5 bar / 1200 K, cavity pressure at station "p_Inj_1"

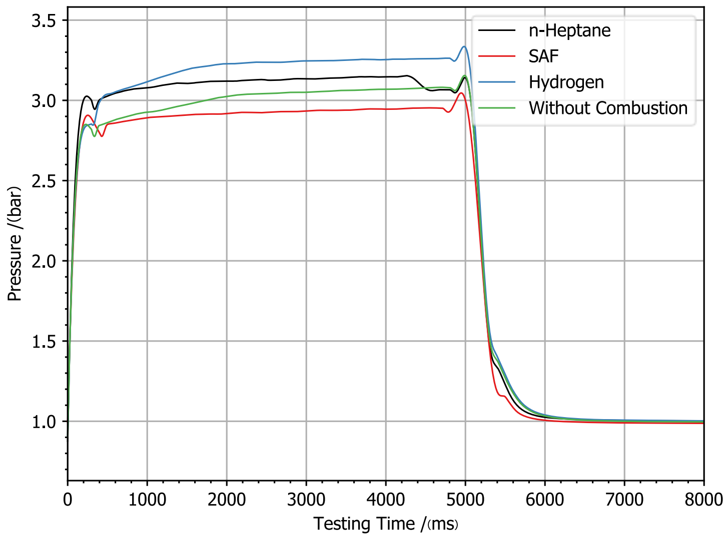

Fig 9. 5 bar / 1200 K, ramp pressure at station "p_Inj_2"

Figure 8 compares the static pressure distributions for all three different fuels versus the case without combustion at station "p_Inj_1" (refer to Fig. 4). This pressure measurement station is located about 10 mm downstream of the injector element. Without combustion a maximum static pressure of 3.25 bar is reached. The combustion of SAF results in a similar pressure slightly lower than that (3.1 bar). A pressure rise to the pressure without combustion at the end of the run indicates that the lower static pressure is caused by the SAF combustion process. 500 ms before the end of the run the glowing plug is switched off resulting in a collapse of the fuel combustion in case of SAF and slightly later in case of hydrogen. For n-heptane the static pressure reaches 3.4 bar before the combustion process ends around 4.5 s into the run which causes the temperatures (refer to Figures 6 and 7) and the pressure (see Fig. 8) to drop. The highest static pressure in the cavity is reached in the hydrogen case (around 3.7 bar).

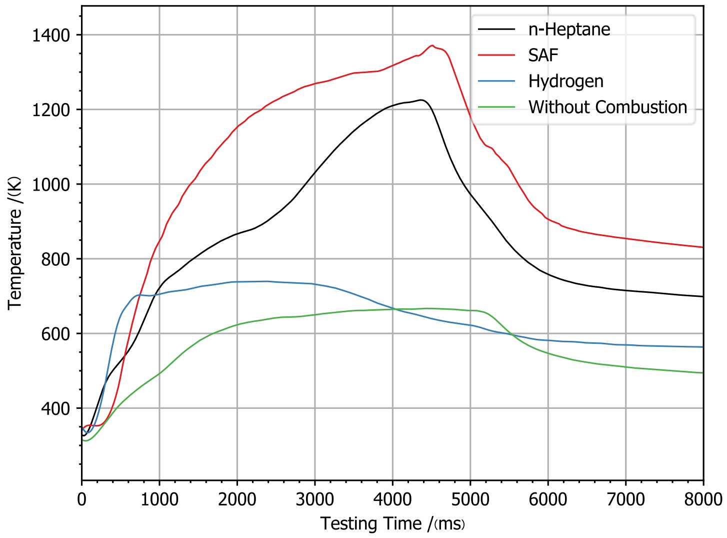

Fig 10. 7 bar / 1200 K, cavity temperature at station "T_Inj_1"

Figure 9 displays the static pressure distributions for the different fuels at station "p_Inj_2" (refer to Fig. 4) for the 5 bar / 1200 K boundary condition. The distribution of the pressure graphs is similar to Fig. 8 but all pressure values are reduced 0.5 bar compared to the cavity pressures. Figure 10 shows the temperature distribution in the cavity for the tested fuels at the 7 bar / 1200 K boundary condition. At this boundary condition the combustion of SAF creates the highest temperatures in the cavity (1350 K in Fig. 10 instead of 780 K in Fig. 6). The higher wall temperatures in the cavity are caused by a higher stagnation pressure of the air vitiator which results in a stronger intrusion of the hot gas main flow into the cavity, thus providing more oxidiser. For n-heptane the increase in temperature compared to the 5 bar / 1200 K case is less significant (1200 K in Fig. 10 vs. 1050 K in Fig. 6). In case of hydrogen the temperature reaches 750 K before it drops to 600 K, which is below the wall temperature without combustion (around 650 K).

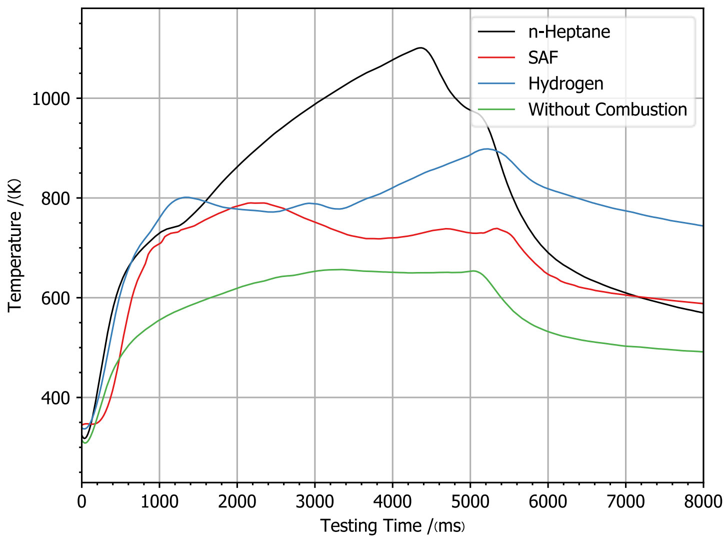

Fig 11. 7 bar / 1200 K, ramp temperature at station "T_Inj_2"

However, in Fig. 11 it is obvious that the temperature at the ramp rises for hydrogen at the moment where it drops in the cavity. This indicates a shift in position of the flame / combustion zone further downstream. For the ramp region in Fig. 11 its temperature graph is similar to Fig. 7, but with a slightly higher maximum temperature of 900 K (Fig. 11) vs. 880 K (Fig. 7). So, for hydrogen the stronger intrusion of the hot gas main flow raises the temperature in the cavity, but not in the combustion zone at the ramp. With n-heptane as a fuel, the temperature at the ramp reaches 1100 K (Fig. 11) vs. 975 K (Fig. 7). For SAF the temperature at the ramp reaches up to 790 K (Fig. 11) vs. 650 K in Fig. 7. This results in a hotter combustion with more downstream position of the combustion zone, but still the main combustion happens within the cavity (see Fig. 10). At the ramp the temperatures without combustion are comparable to the previous case (refer to Fig. 7).

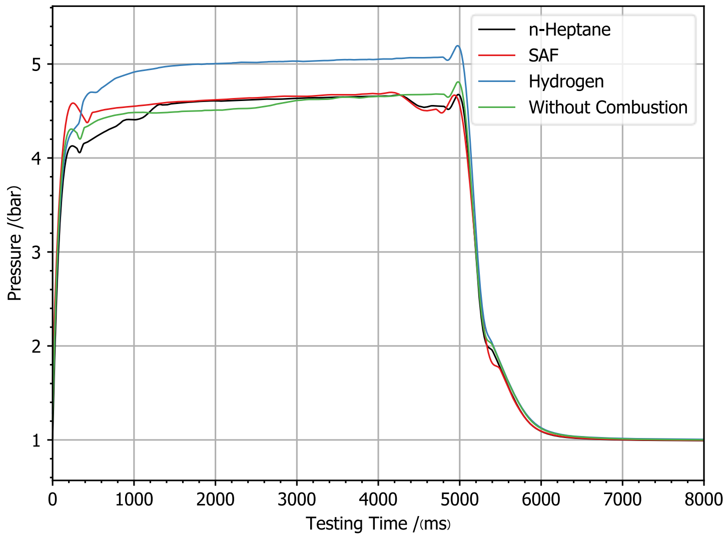

Fig 12. 7 bar / 1200 K, cavity pressure at station "p_Inj_1"

In Fig. 12 the pressure distributions are compared for the 7 bar / 1200 K case at the cavity station ("p_Inj_1" in Fig. 4). For all fuels higher pressures are reached compared to Fig. 8, which is mainly caused by a higher stagnation pressure at this boundary condition. In contrast to the 5 bar / 1200 K case, n-heptane features the same pressure as SAF and without combustion. However, hydrogen combustion increases the cavity pressure to 5 bar.

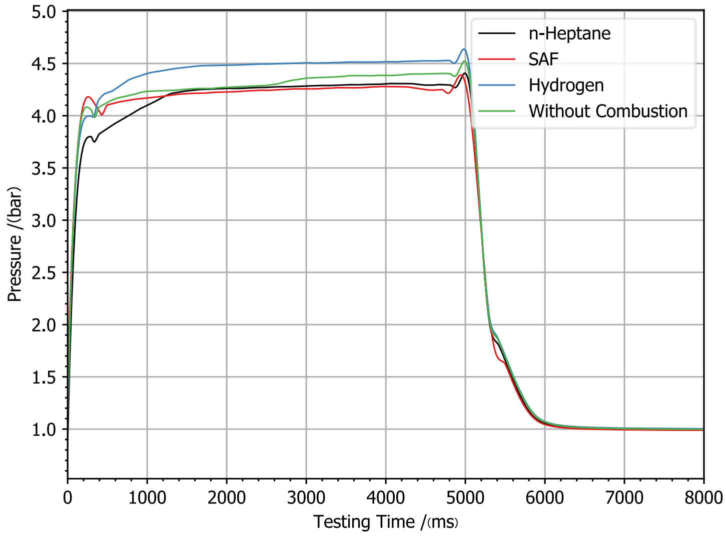

Fig 13. 7 bar / 1200 K, ramp pressure at station "p_Inj_2"

The same can be observed at the ramp station downstream (see Fig. 13), where hydrogen also is the only fuel that leads to a significant pressure increase compared to the reference case. This indicates that the combustion zones introduce heat into the wall region, but also increase their distance to the wall, so that they less affect the pressure distribution.

Figures 14 to 17 only compare the two tested hydrocarbons as no hydrogen test runs with a fuel mass flow rate of 1.50 g/s could achieve sustainable combustion at this air vitiator condition (see [9]). At the 9 bar / 1200 K boundary condition, SAF causes a cavity wall temperature maximum of 1500 K (see Fig. 14), whereas in the 7 bar / 1200 K case 1350 K is reached (see Fig. 10). A higher maximum also applies for n-heptane with 1350 K vs. 1200 K. In Fig. 14 the thermocouple failed during the reference run, thus the reference is not valid in this case.

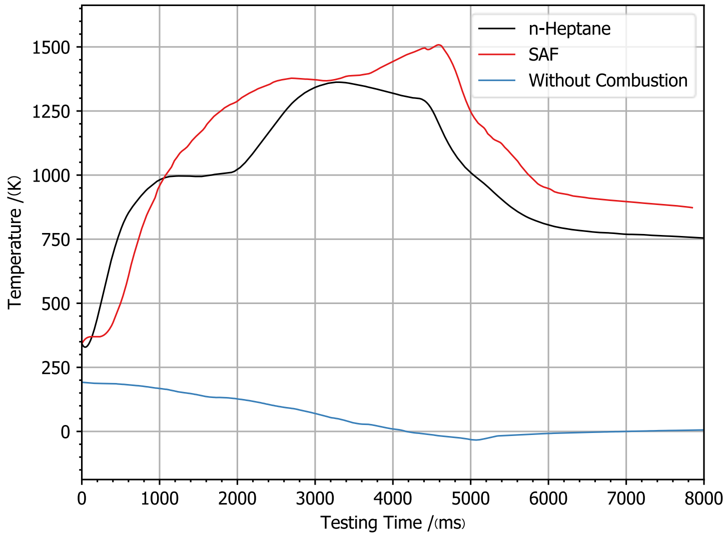

Fig 14. 9 bar / 1200 K, cavity temperature at station "T_Inj_1"

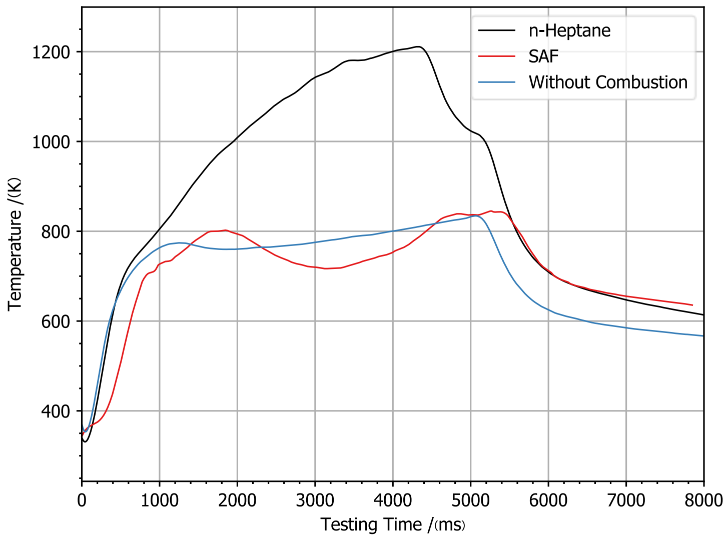

Fig 15. 9 bar / 1200 K, ramp temperature at station "T_Inj_2"

At the ramp, the wall temperature reaches 1200 K for n-heptane (see Fig. 15) in contrast to the 7 bar / 1200 K case in Fig. 11. This is 100 K higher than in Fig. 11. SAF fuel introduces a wall temperature similar to the one without combustion in Fig. 15. Between 1800 and 4700 ms the temperature graph for the case without combustion is undercut. This indicates, as in the previous cases, a strong focus of the combustion zone on the cavity. Additionally, the hot gases from the combustion zone move away from the wall at the ramp causing the significant undershooting of the temperature. This is supported by Fig. 16 and 17 which display the wall pressure distribution at the cavity and at the ramp respectively. Both figures show pressure distributions close to the case without combustion. Thus, an effect on the wall pressure decreases with increasing stagnation pressure.

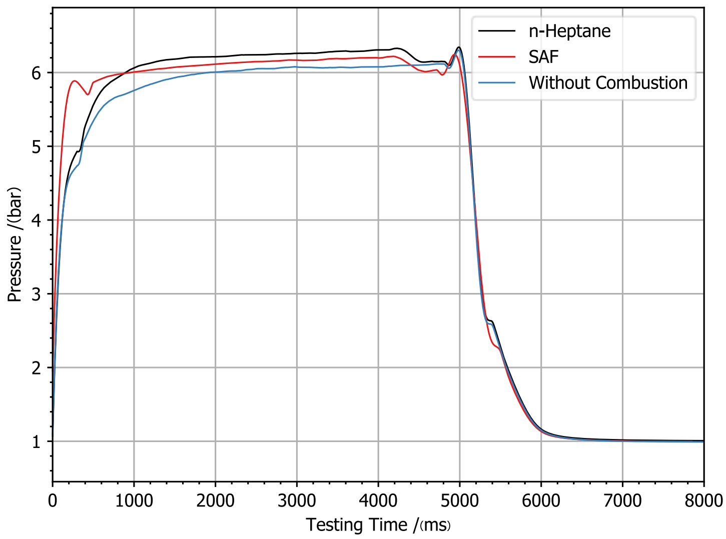

Fig 16. 9 bar / 1200 K, cavity pressure at station "p_Inj_1"

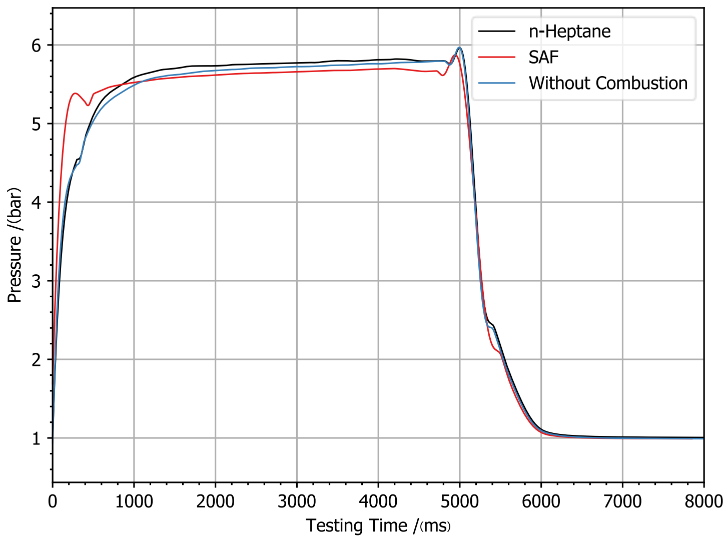

Fig 17. 9 bar / 1200 K, ramp pressure at station "p_Inj_2"

5. Conclusions

DLR Lampoldshausen has conducted more than 400 hot gas test runs at its M11.1 chemical air vitiator test bench for the H2020 project More&Less. The scope of those experiments was a better insight into combustion and emission processes for a Ramjet operated with hydrogen and sustainable aviation fuels (SAF) / bio fuels. The current publication analysed selected topics from those experimental test campaigns by comparing the exhaust gas composition for the different hydrocarbons and the temperature and pressure distributions within the injector cavity for all three fuels. The exhaust gas compositions were very similar between n-heptane and SAF. However, unburned hydrogen could be detected at all boundary conditions with n-heptane as a fuel. Reference measurements at the air vitiator did not detect any hydrogen in the vitiated air, thus the source is most likely the n-heptane combustion process at the model combustion chamber. Analyses of the temperature and pressure distribution at the injector indicate different positions of the flame / combustion zone for the different fuels driven by the different air vitiator boundary conditions. For n-heptane the combustion caused the highest temperatures at the 5 bar and 9 bar boundary conditions with a combustion zone location slightly downstream of the main cavity. SAF combusted almost entirely within the cavity, whereas hydrogen combusted mostly downstream of the cavity. With increasing stagnation pressure, the static wall pressure in the injector region is less affected by the combustion process. In contrast the static wall temperature generally rises with increasing stagnation pressure due to a better availability of oxidiser from the hot gas main flow. Those findings correspond well with the numerical simulations performed by partner organisations within the More&Less project, but the detailed combustion process needs further clarification and investigation.

6. Outlook

Additional analyses of the obtained data are necessary. Especially the detailed combustion process and the reason for the hydrogen findings within the exhaust gas are not yet fully understood. Future publications will put this into context with a visual flame analysis and additional investigations of the influence of different fuel mass flow rates on the pressure and temperature distribution at the injector. Future publications are also planned to include a detailed comparison between numerical simulation data and experimental data to gain a better understanding of the combustion and emission processes.

Acknowledgements

The work presented in this paper is funded by the Horizon 2020 Program of the European Commission under Grant Agreement GA-101006856. This support and the gas sampling support by DLR's department CTT is greatly appreciated by the authors.

References

1. Sholto, F., Smart, M. K., Kearney, M. P., Jahn, I.: Flyback of the SPARTAN Scramjet-Powered Launch Vehicle. AIAA- American Institute of Aeronautics and Astronautics, AIAA 2018-2177 (2018). https://doi.org/10.2514/6.2018-2177
2. Kerst, A., Gross, K. C., Oren, E. P., Komives, J. R., Rhoby, M., Ombrello, T.: Preliminary Investigation of a Scramjet Flowfield with Hyperspectral Imaging. AIAA- American Institute of Aeronautics and Astronautics, AIAA 2017-4646 (2017). https://doi.org/10.2514/6.2017-4646
3. Speier, R., Nacouzi, G., Lee, C., Moore, R.: Hypersonic Missile Nonproliferation - Hindering the Spread of a New Class of Weapons. RAND Corporation, RR-2237-CC (2017). https://doi.org/10.7249/RR2137
4. Strauss, F., General, S., Manfletti, C., Schlechtriem, S.: Flow Visualizations with Background Oriented Schlieren in a Transpiration-Cooled Model Scramjet Combustor. Int. J. of Energetic Mat. and Chem. Prop. 18(2), 133-155 (2019). https://doi.org/10.1615/IntJEnergeticMaterialsChemProp.2019028003
5. Strauss, F., Manfletti, C., Lieberwirth, R. and Schlechtriem, S., "Experimental Setup on Transpiration Cooling in Supersonic Combustion Ramjets (Scramjets)," 5th Space Propulsion Conference, 2nd to 6th May 2016, Rome, Italy, (2016).
6. Strauss, F., Manfletti, C., Freudenmann, D., Witte, J., Schlechtriem, S.: Preliminary Experiments on Transpiration Cooling in Ramjets and Scramjets. AIAA- American Institute of Aeronautics and Astronautics, AIAA 2016-4968, (2016). https://doi.org/10.2514/6.2016-4968
7. Strauss, F., General, S., Cragg, P., Schlechtriem, S.: Wall Pressure Stability and Cooling Efficiency Analysis in a Transpiration-Cooled Scramjet Model Combustor. HiSST:2nd International Conference on High-Speed Vehicle Science Technology, 11-15 September 2022, Bruges, Belgium. HiSST-2022-0007.
8. Settles, G. S., Hargather, M.: A Review of Recent Developments in Schlieren and Shadowgraph Techniques. Meas. Science and Techn. 28, 042001, (2017). https://doi.org/10.1088/1361-6501/aa5748
9. Strauss, F., Manassis, K., Wilhelm, M., Kirchberger, C.: Experiments on High Speed Air-Breathing Propulsion for Sustainable Supersonic Flight. HiSST:3rd International Conference on High-Speed Vehicle Science Technology, 14-19 April 2024, Busan, Korea (2024).
10. Dambowsky, F., A Perfect Duet, In: DLRmagazine No. 157, DLR German Aerospace Center, Cologne, pp. 8-15, April 2018 (2018).
11. Strauss, F., Manassis, K., Bauer, L.., Kirchberger, C.: Experiments on Ramjet Combustion Emissions for Sustainable Supersonic Flight. 3rd International Conference on Flight vehicles, Aerothermodynamics and Re-entry (FAR), 18-22 May 2025, Arcachon, France (2025).

